Chinese Chemical Letters 31 (2020) 1387–1391

Contents lists available at ScienceDirect

Chinese Chemical Letters

journal homepage: www.elsevier.com/locate/cclet

Communication

Design of high stability thin-film transistor biosensor for the diagnosis of bladder cancer

Yingxue Li[a,1], Bo Zeng[a,1], Yujie Yang[a], Huageng Liang[c,**], Yanbing Yang[a,b,d,*], Quan Yuan[a,b,*]

[a] Key Laboratory of Analytical Chemistry for Biology and Medicine (Ministry of Education), College of Chemistry and Molecular Sciences, Wuhan University, Wuhan 430072, China
[b] Institute of Chemical Biology and Nanomedicine, State Key Laboratory of Chemo/Biosensing and Chemometrics, College of Chemistry and Chemical Engineering, Hunan University, Changsha 410082, China
[c] Department of Urology, Union Hospital, Tongji Medical College, Huazhong University of Science and Technology, Wuhan 430022, China
[d] Key Laboratory for Micro-/Nano-Optoelectronic Devices of Ministry of Education, School of Physics and Electronics, Hunan University, Changsha 410082, China

ARTICLE INFO

Article history:
Received 14 January 2020
Received in revised form 9 March 2020
Accepted 15 March 2020
Available online 18 March 2020

Keywords:
IGZO
Field-effect transistors
NMP22
Bladder cancer
Urine detection

ABSTRACT

Bladder cancer is the most common malignant tumor in the urinary system, with high morbidity, mortality and recurrence after surgery. However, current bladder cancer urine diagnosis methods are limited by the low accuracy and specificity due to the low abundance of bladder cancer biomarkers in the urine with complex biological environments. Herein, we present a high stability indium gallium zinc oxide field effect transistor (IGZO-FET) biosensor for efficient identification of bladder cancer biomarkers from human urine samples. The recognition molecular functionalized IGZO-FET biosensor exhibits stable electronic and sensing performance due to the large-area fabrication of IGZO thin-film FET. Owing to the excellent electrical performance of IGZO-FET, the IGZO-FET biosensor exhibits high sensitivity and extremely low detection limit (2.7 amol/L) towards bladder cancer biomarkers. The IGZO-FET biosensor is also able to directly detect bladder tumor biomarker in human urine with high sensitivity and specificity, and could differentiate bladder cancer patients' urine samples from healthy donors effectively. These results indicate that our designed high-performance biosensor shows great potential in the application of portable digital bladder cancer diagnosis devices.

Bladder cancer is one of the most common urogenital malignant tumors with extremely high morbidity, mortality and easy recurrence after surgery [1,2]. The pathological pattern of bladder cancer is complex, and it is difficult to identify [3]. Currently, cystoscopy is the gold standard for clinical diagnosis of bladder cancer, but is an uncomfortable and costly invasive procedure, even associated with urinary tract infections and different levels of hematuria [4,5]. Since the metabolic environment of bladder tumor cells is urine, their direct or induced metabolites will remain in the urine. Some of the metabolites such as telomerase, nuclear matrix protein and bladder tumor antigen have been identified as biomarkers of bladder tumor [6–9]. In this regard, the bladder cancer liquid biopsy technology would provide a new way for the painless and noninvasive diagnosis of bladder cancer [10,11]. However, because of the complex urine composition and low abundance of biomarkers, the achievement of high sensitivity and accuracy detection of bladder cancer is significantly limited.

Recently, field effect transistors (FETs) have been applied to a variety of biosensors because of their extraordinary electronic characteristics, such as fast response, miniaturization and circuit integration [12–15]. The FET-based biosensor can simultaneously serve as a sensor and an amplifier, causing an obvious channel current change under a tiny voltage variation, in which high sensing sensitivity can be attained [16,17]. At present, FETs based on indium gallium zinc oxide (IGZO-FETs) have attracted great attention due to the features of simple preparation process, large-scale fabrication, array formation and high signal stability, and over the past decades, IGZO-FETs have been widely employed to

* Corresponding authors at: Key Laboratory of Analytical Chemistry for Biology and Medicine (Ministry of Education), College of Chemistry and Molecular Sciences, Wuhan University, Wuhan 430072, China.
** Corresponding author.
E-mail addresses: leonard19800318@hust.edu.cn (H. Liang), yangyanbing@whu.edu.cn (Y. Yang), yuanquan@whu.edu.cn (Q. Yuan).
[1] These authors contributed equally to this work.

https://doi.org/10.1016/j.cclet.2020.03.043

develop commercial displays and nano-biosensors [18–22]. It is anticipated that the fabrication of a large-area FET array device for highly sensitive detection and accurate analysis of bladder tumor biomarkers is a hopeful method to achieve early-stage noninvasive diagnosis of bladder cancer.

Herein, we present an IGZO-FET biosensor for quantitative detection of bladder cancer biomarkers from human urine samples with high stability and sensitivity. The IGZO-FET biosensor functionalized by nuclear matrix protein 22 (NMP22) antibody exhibits reliable and sensitive electronic performance due to the fabrication of uniform and smooth IGZO thin-film and the specific combination of antibody-antigen. We demonstrate that the fabricated IGZO-FET biosensor could quantify NMP22 concentration down to detection limit of 0.0001 pg/mL. Besides, the IGZO-FET biosensor can be applied to directly quantify bladder cancer biomarkers in human urine and differentiate bladder cancer patients' urine samples from healthy donors.Our designed high-performance biosensor promises a candidate for potential applications in postoperative monitoring, therapeutic evaluation, and personal health management.

The IGZO-FET biosensor array is schematically illustrated in Scheme 1, in which each FET was composed of a Si/SiO_2 wafer substrate, IGZO sensing channel layer, and source/drain electrodes. For the preparation of IGZO-FET biosensor array, patterned metallic electrodes (15 nm Cr/50 nm Au) were first deposited as source/drain electrodes through photolithography and thermal evaporation on the wafer substrate (1 cm × 1 cm Si/SiO_2 wafer). Next, a 20 nm thick IGZO (In_2O_3:Ga_2O_3:ZnO = 1:1:1) sensing channel was deposited on the patterned metallic electrodes by RF sputtering *via* a shadow mask (Fig. S1 in Supporting information). For the functionalization of IGZO-FET array, a poly (methylmethacrylate) (PMMA) protection layer was first spin-coated on the surface of IGZO layer to passivate the Cr/Au source drain electrode, and to eliminate the contact resistance and avoid leakage current between the source/drain electrode and the sensing channel in the sensing measurements. Next, the IGZO sensing region was exposed by photolithographic process, and further functionalized by anti-NMP22 through a series of procedures (Experimental Section in Supporting information). In short, the (3-aminopropyl)triethoxysilane (APTES) and glutaraldehyde were used as cross-linking molecules to immobilize antibodies [23], and lastly, the antibody functionalized IGZO sensing region was incubated with Bovine Serum Albumin (BSA) to passivate the sensing surface to reduce non-specific adsorption.

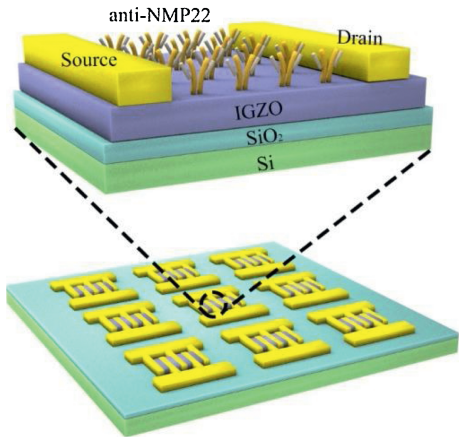

Scheme 1. Schematic illustration of the fabrication of anti-NMP22 functionalized IGZO-FET biosensor array.

The fundamental structural and electrical characteristics of the IGZO-FET are shown in Fig. 1 and Fig. S2 (Supporting information). The scanning electron microscopy image of the IGZO thin film clearly indicates the smooth surface of the uniform IGZO layer and the thickness of IGZO layer is about 20 nm (Fig. 1a). The drain current-gate voltage, I_d-V_g transfer curve was measured in air and at the drain voltage (V_d) of 1 V (Fig. 1b). The field effect mobility (μ_{FE}) was calculated using the following equation to evaluate the performance of IGZO-FET [24,25]:

$$\mu_{FE} = \frac{g_m L}{W V_d C_{ox}} = \frac{dI_d}{dV_g} \frac{L}{W V_d C_{ox}}$$

where L and W are the channel length (80 μm) and width (240 μm), C_{ox} is capacitance per unit area, and g_m is the transconductance of IGZO-FET. The maximum value of g_m obtained by the I_d-V_g curve is 0.0025 mS. Consequently, the calculated μ_{FE} of the FET with 20 nm IGZO channel is 24.2 $cm^2\ V^{-1}\ s^{-1}$, which is the highest μ_{FE} among the prepared FETs with different thickness of IGZO channel layers by controlling sputtering time (Fig. S3 in Supporting information). It indicates that the prepared IGZO-FET exhibits excellent electrical properties. Furthermore, in order to investigate the stability of the IGZO-FET device, we carried out electrical performance tests on nine IGZO-FETs on the same Si/SiO_2 substrate (Fig. 1c). It can be seen that the I_d-V_g transfer curves originated from different IGZO-FET devices are basically consistent, indicating that the IGZO-FET devices exhibit stable electrical performance. The excellent electrical stability of IGZO-FET is due to the uniform IGZO layer over large-area. The above results demonstrate that the IGZO-FET arrays show excellent electrical performance and confirm its application in accurate and stable sensing.

The sensing performance of IGZO-FET biosensor towards bladder cancer biomarkers was then investigated. The modification of antibody molecules on IGZO-FET is schematically illustrated in Fig. 2a, and the morphology and structure of IGZO-FET biosensor was first investigated. The successful surface functionalization of IGZO-FET can be clearly identified by atomic force microscopy (AFM) images (Figs. 2b and c). It is observed that the bare IGZO film is uniform over large-area, which agrees with the SEM images (Fig. 1a). In comparison, the surface roughness of anti-NMP22 conjugated IGZO film increased distinctly, suggesting that the antibody molecules were effectively attached to the IGZO surface. The anti-NMP22 molecules modified on the IGZO-FET specifically interacts with target NMP22 molecules and then generates an electrical signal change on the biosensor, thus realizing the specific detection (Fig. 3a). The NMP22 aqueous solution acts as gate dielectric and Ag/AgCl electrode serves as the gate electrode ($V_{Ag/AgCl}$). Fig. 3b shows the I_d-V_g transfer characteristics of IGZO-FET biosensor when exposed to NMP22 solutions with different concentrations. It appears that the IGZO-FET biosensor exhibits a consistent decrease in source-drain current with increasing concentration of NMP22 solutions. This observation in channel current variation can be attributed to the NMP22 protein binding reaction. Specifically, negatively charged NMP22 protein is specifically linked to its antibody and forms a complex on the surface of IGZO channel, which is equivalent to a negative gate on the channel surface. This causes a decrease in the carrier density and conductance of IGZO channel and a more positive $V_{Ag/AgCl}$ is required to obtain the same initial current. Along with the amount of NMP22 protein binding to the sensing area of IGZO surface increases, the applied negative gate effect gradually strengthens, inducing the decrease of carrier density and thus the current of the IGZO-FET biosensor under the same $V_{Ag/AgCl}$. The ratio of drain current change (ΔI_d) to initial value (I_0) *versus* NMP22 concentration (C_{NMP22}) is plotted in Fig. 3c. As shown in the curve, $\Delta I_d/I_0$ exhibits a sharp increase when $C_{NMP22}$is increased from

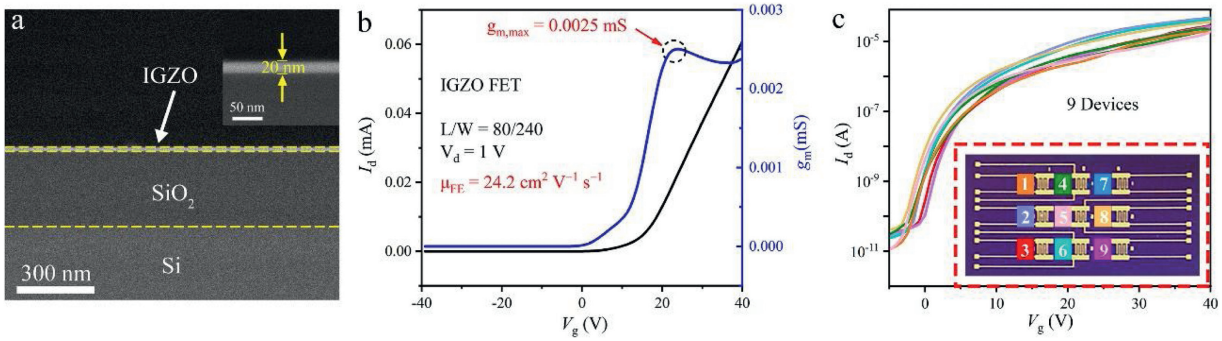

Fig. 1. (a) Cross-section SEM image of the IGZO-FET. Inset: Enlarged SEM image of the IGZO layer. (b) Transfer curve and transconductance curve of the back-gated IGZO-FET device at V_d = 1 V. (c) Stability of the back-gated IGZO-FET device at V_d = 1 V. Inset: Photograph of the IGZO-FET array.

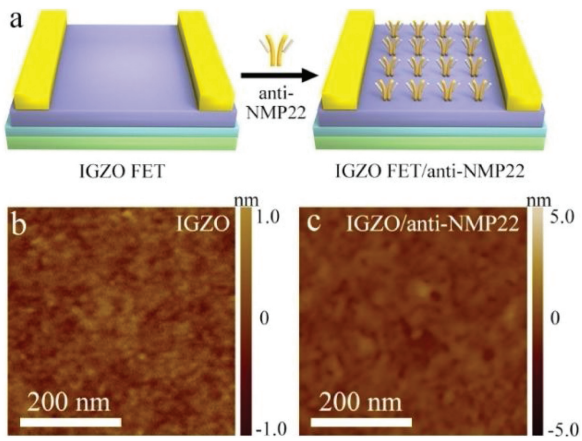

Fig. 2. (a) Schematic illustration of IGZO-FET biosensor functionalized by anti-NMP22. AFM images of IGZO thin-film (b) before and (c) after anti-NMP22 modification.

0.0001 pg/mL, and finally becomes saturated. The linear detection range is 0.0001∼0.1 pg/mL. In addition, in order to evaluate the accuracy of the IGZO-FET biosensor, the recovery rate of this method was calculated. As shown in Table S1 (Supporting information), the recovery ranges from 96.2%–110.9% over the linear operating range, suggesting that the IGZO-FET biosensor can be employed to precisely evaluate the NMP22 target molecules in human urine samples.

The real-time electrical response of IGZO-FET biosensor towards NMP22 proteins was then investigated. The schematic diagram of dynamic sensing measurement is shown in Fig. S4 (Supporting information). Different concentrations of NMP22 solution were passed into IGZO-FET at a fixed rate of 0.1 mL/min. From Fig. 3d, it can be seen that the sensing current variation increases with increasing concentrations of NMP22 protein and the response speed (5 s) is very fast, suggesting that the anti-NMP22 molecules modified IGZO-FET biosensor exhibits high sensitivity. It is also observed that a 0.0001 pg/mL NMP22 solution causes an obvious current change (1.5 μA), suggesting that the lowest detection limit of the IGZO-FET biosensor for NMP22 protein is 2.7 amol/L, which is much lower than

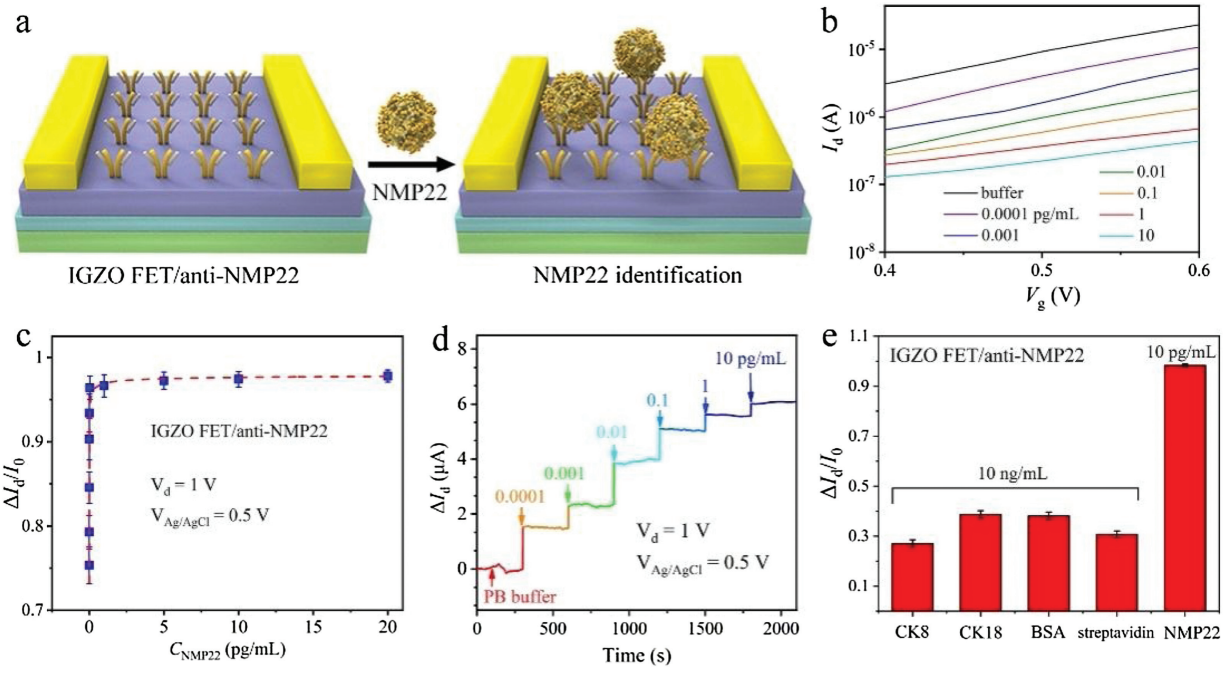

Fig. 3. (a) Schematic illustration of the specific detection of bladder cancer biomarkers with IGZO-FET biosensor. (b) Transfer characteristics of solution-gated IGZO-FET biosensor in response to different C_{NMP22} (0.0001–10 pg/mL) at V_d = 1 V. (c) Current variation ($\Delta I_d/I_0$) of IGZO-FET biosensor *versus* C_{NMP22}. (d) Real-time electrical response of anti-NMP22 modified IGZO-FET biosensor towards different C_{NMP22}. (e) Current variation of the anti-NMP22 modified IGZO-FET biosensor in response to nonspecific protein (CK8, CK18, BSA, streptavidin) and specific NMP22 protein. All the error bars represent the standard deviations of three measurements.

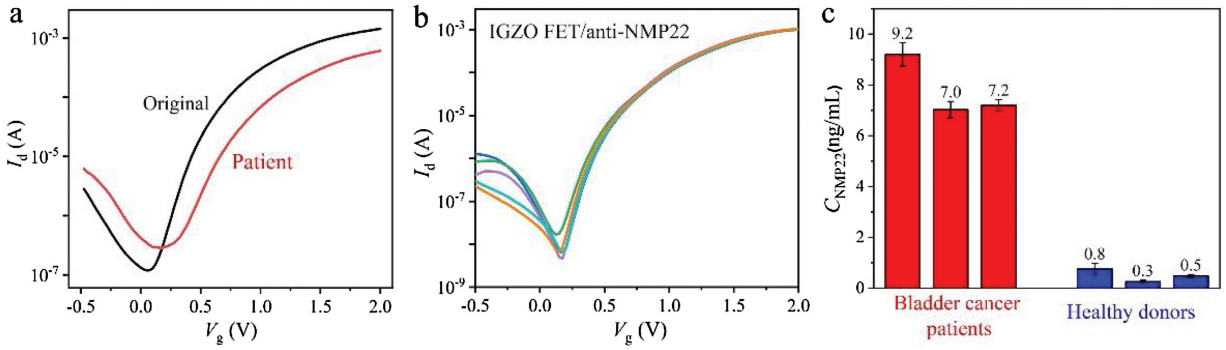

Fig. 4. (a) Transfer characteristics of solution-gated anti-NMP22 modified IGZO-FET biosensor in response to NMP22 protein in urine samples from bladder cancer patients. The V_d is set at 1 V. (b) Transfer characteristics of five solution-gated anti-NMP22 modified IGZO-FET biosensors in response to urine samples from a same bladder cancer patient. The V_d is set at 1 V. (c) Evaluation of the sensing performance of anti-NMP22 modified IGZO-FET biosensor in response to urine samples from bladder cancer patients and healthy donors. The error bars represent the standard deviations of three measurements.

the concentration of NMP22 protein in the urine of bladder cancer patients (nmol/L level) [26,27]. In addition, control experiments were carried out to investigate the specificity and selectivity of our designed IGZO-FET biosensor (Fig. 3e). It can be seen that a low concentration (10 pg/mL) of NMP22 solution causes a significant current response, while the biosensor only exhibits a negligible current change when treated with high concentration (10 ng/mL) of nonspecific proteins solution (cytokeratin 8 (CK8), cytokeratin 18 (CK18), bovine serum albumin (BSA) and streptavidin). These results indicate that the IGZO-FET biosensor provides a high selective recognition ability to target proteins and low binding affinity to nonspecific molecules, further ensuring the application of biosensors to detect target molecules in complex environments.

To investigate the applicability of the IGZO-FET biosensor in clinical diagnosis, a further test with real urine samples was performed. As shown in Fig. 4a, there is a significant change in the current signal when the biosensor was subjected to urine samples from bladder cancer patients. Besides, similar results were obtained when five anti-NMP22 modified IGZO-FET biosensors were employed to test the same patient's urine sample simultaneously (Fig. 4b). These measurements verify that the prepared IGZO film is uniform over large area, and this uniformity is necessary to ensure the reproducibility and reliability of IGZO-FET biosensor. The amounts of NMP22 protein in urine samples from different individuals were further detected and calculated according to the linear relationship of $\Delta I_d/I_0$ *versus* C_{NMP22} (Fig. 4c and Fig. S5 in Supporting information). It is worth mentioning that the urine samples were diluted to ensure that the concentration of NMP22 located in the linear detection range of our IGZO-FET biosensor. It can be seen that the protein concentration in urine from the bladder cancer patients are much higher than those from healthy donors. Additionally, the sensing performance of our IGZO-FET biosensor is generally consistent with the traditional ELISA method (Table S2 in Supporting information), indicating that the IGZO-FET biosensor shows great potential for application in bladder cancer diagnostics.

In conclusion, we have designed a recognition molecular conjugated IGZO-FET biosensor to detect bladder tumor biomarker in real urine samples. The prepared IGZO thin film is homogeneous and uniform over large-area. This uniform structure enables a stable electrical signal of IGZO-FETs. After modification with anti-NMP22, the IGZO-FET biosensor is able to detect NMP22 protein with high sensitivity and selectivity, and the detection limit is down to amol/L level. More importantly, our fabricated IGZO-FET biosensor can be applied to monitor target molecules in complex urine samples, and to differentiate the urine samples from bladder cancer patients and healthy donors by quantifying the amount of NMP22 protein. This design of high performance IGZO-FET biosensor suggests a strategy to realize early-stage bladder cancer digital diagnosis.

Declaration of competing interest

The authors declare that they have no known competing financial interests or personal relationships that could have appeared to influence the work reported in this paper.

Acknowledgments

This work was supported by the National Key Research and Development Program of China (No. 2017YFA0208000), the National Natural Science Foundation of China (Nos. 21925401, 21904033, 21675120), and Changsha Municipal Science and Technology Projects, China (No. kq1901030).

Appendix A. Supplementary data

Supplementary material related to this article can be found, in the online version, at doi:https://doi.org/10.1016/j.cclet.2020.03.043.

References

[1] A.K. Schneider, M.F. Chevalier, L. Derré, Nat. Rev. Urol. 16 (2019) 613–630.
[2] S. Antoni, J. Ferlay, I. Soerjomataram, A. Znaor, A. Jemal, F. Bray, Eur. Urol. 71 (2017) 96–108.
[3] B.W.G. van Rhijn, H.G. van der Poel, T.H. van der Kwast, Eur. Urol. 47 (2005) 736–748.
[4] X. Zhang, Y. Zhang, X. Liu, et al., Oncotarget 7 (2015) 3255–3266.
[5] S. Goodison, C.J. Rosser, V. Urquidi, Mol. Diagn. Ther. 17 (2013) 71–84.
[6] A. Mitra, R. Cote, Nat. Rev. Urol. 7 (2010) 11–20.
[7] S. Jeong, Y. Park, Y. Cho, Y.R. Kim, H. Kim, Clin. Chim. Acta 414 (2012) 93–100.
[8] K.K. Pasikanti, K. Esuvaranathan, P.C. Ho, et al., J. Proteome Res. 9 (2010) 2988–2995.
[9] A. Sreekumar, L. Poisson, T. Rajendiran, et al., Nature 457 (2009) 910–914.
[10] G. Siravegna, S. Marsoni, S. Siena, et al., Nat. Rev. Clin. Oncol. 14 (2017) 531–548.
[11] E. Crowley, F.D. Nicolantonio, F. Loupakis, A. Bardelli, Nat. Rev. Clin. Oncol. 10 (2013) 472–484.
[12] S. Zhang, R. Geryak, J. Geldmeier, et al., Chem. Rev. 117 (2017) 12942–13038.
[13] M. Zhou, S. Dong, Acc. Chem. Res. 44 (2011) 1232–1243.
[14] S. Cheng, S. Hideshima, S. Kuroiwa, T. Nakanishi, T. Osaka, Sens. Actuators B 212 (2015) 329–334.
[15] D. Li, L. Liang, Y. Tang, et al., Chin. Chem. Lett. 30 (2019) 1013–1016.
[16] F. Yan, M. Zhang, J. Li, Adv. Healthcare Mater. 3 (2013) 313–331.
[17] Y.B. Yang, X.D. Yang, X.M. Zou, et al., Adv. Funct. Mater. 27 (2017)1604096.
[18] J.C. Chou, M.S. Huan, Y.H. Liao, et al., Mater. Lett. 176 (2016) 94–96.
[19] X. Yu, T.J. Marks, A. Facchetti, Nat. Mater. 15 (2016) 383–396.
[20] H. Chen, Y. Cao, J. Zhang, et al., Nat. Commun. 5 (2014) 4097.

[21] X. Du, Y. Li, J.R. Motley, et al., ACS Appl. Mater. Interfaces 8 (2016) 7631–7637.
[22] Y. Cui, Q. Wei, H. Park, C.M. Lieber, Science 293 (2001) 1289–1292.
[23] H. Chen, Y.S. Rim, I.C. Wang, et al., ACS Nano 11 (2017) 4710–4718.
[24] T. Kamiya, K. Nomura, H. Hosono, Sci. Technol. Adv. Mater. 11 (2010)044305.
[25] A. Abliz, D. Wan, J.Y. Chen, et al., IEEE T. Electron. Dev. 20 (2018) 1–6.
[26] S. Jeong, Y. Park, Y. Cho, et al., Clin. Chim. Acta 414 (2012) 93–100.
[27] M.H. Lee, J.L. Thomas, Y.C. Chang, et al., Biosens. Bioelectron. 79 (2016) 789–795.